

Received 26 June 2023, accepted 16 July 2023, date of publication 20 July 2023, date of current version 28 July 2023.

Digital Object Identifier 10.1109/ACCESS.2023.3297217

## RESEARCH ARTICLE

# A High Gain and Uniform Power Mushroom Antenna Using Metasurface

DANH MANH NGUYEN<sup>1</sup>, DUCDUNG NGUYEN<sup>1</sup>, (Graduate Student Member, IEEE),  
AND CHULHUN SEO<sup>1</sup>, (Senior Member, IEEE)

Department of Information and Communication Convergence, Soongsil University, Seoul 06978, South Korea

Corresponding author: Danh Manh Nguyen (nguyendanhmanh1998@gmail.com)

This work was supported by the Basic Science Research Program through the National Research Foundation of Korea (NRF) funded by the Ministry of Science and ICT under Grant NRF-2017R1A5A1015596.

**ABSTRACT** In this study, we present a simple feed-aperture coupled antenna with a high gain and flat-top radiation pattern for microwave power transmission (MPT) applications involving misalignment. A  $4 \times 4$  mushroom structure is proposed to suppress the back-lobe radiation and to achieve the high gain of the aperture-coupled antenna. Additionally, to improve the flat-top radiation pattern and circular polarization (CP), an array  $4 \times 4$  metasurface is employed to obtain an equal electric field in the propagation direction. The overall dimensions are  $2.13\lambda_0 \times 2.13\lambda_0 \times 0.228\lambda_0$  at 5.8 GHz. The measurement results show that the impedance bandwidth of  $< -10$  dB of 5.5 - 6 GHz (8.69 %), a maximum realized left-hand circular polarization (LHCP) gain of 10.4 dBi with flat-top beamwidth (1-dB) of  $36^\circ$  and  $38^\circ$  for E and H plane, respectively. Moreover, the proposed transmitter antenna is tested in a realistic MPT indicating an advantage of radiating uniform power of 10 mW in the diameter range of 80 mm.

**INDEX TERMS** Circular polarization (CP), flat-topped radiation pattern (FTRP), microwave power transmission (MPT), lateral misalignment, metasurface (MS).

## I. INTRODUCTION

Recently, wireless power transmission (WPT) has advanced rapidly in the communication systems [1], [2], [3], [4]. It can power remote electronic devices where wired charging is difficult or impossible to have access. In this case, the radiation pattern of the antenna has become a necessary characteristic. In practical, the system efficiency is degraded significantly over the long distances, which, as a result, requires a high-gain antenna to achieve high efficiency. The conventional antennas typically exhibit power drop as the angle deviates from the main direction, which limits the application of the conventional antennas in systems where a uniform power level is required over a wide angle range such as WPT, beam steering, and radar.

As an alternative, flat-top radiation pattern (FTRP) antennas have emerged as a promising solution to this limitation because they can offer a nearly constant power level within

The associate editor coordinating the review of this manuscript and approving it for publication was Photos Vryonides<sup>1</sup>.

a certain angle range. With such the unique radiation characteristics, the FTRP antennas have proliferated in wireless communication applications such as satellite communication networks [5], fifth-generation (5G) networks [6], especially microwave power transmission (MPT) systems [7]. Moreover, an FTRP antenna can provide efficient power transfer over a range of distances and orientations, enabling a more flexible position of mobile devices. Besides, in beamforming applications, FTRP can offer a more efficient method of directing the energy to a specific target by reducing the need for the complex beamforming algorithms [8], [9], [10]. Furthermore, it can improve target detection and reduce the effects of sidelobes that can cause interference with other radar systems [11].

Various methods have been conducted to modulate radiation or creation of flat-top beamwidth. For instance, the usage of a Fabry-érot cavity (PFC) antenna based on the ray-tracing model was proposed in [12] and [13] to enhance the gain and especially to obtain the FTRP. Uniform power radiation using leaky wave antennas (LWAs) is also introduced in

literature [14]. Besides, ten-element bowtie dipoles are incorporated with the feeding network to obtain the uniform power from  $-12^\circ$  to  $12^\circ$  [15]. Moreover, circular polarization (CP) can be integrated with the advantage of minimizing losses and offering flexible orientation in the antenna. In [16], a single rectangular dielectric resonator antenna (DRA) combining  $TE_{119}^y$  and  $TE_{113}^y$  modes was designed to obtain flat-top beamwidth of  $85^\circ$  and  $58^\circ$  at E and H planes, respectively. Besides, a flat-top radiation pattern of larger than  $40^\circ$  for both planes and CP is generated by using the mushroom technique [17]. Metasurface (MS) is another potential way to develop antenna efficiency. In one approach, a linear graded index metasurface (LGIMS) lens was constructed to steer the main radiated beam with FTRP characteristics [18]. Another work is to use a small-size double-shell integrated lens antenna [19]. The results show that the MS structure can enhance the gain of the flat-top beam and minimize the antenna's back-lobe, whereas the drawbacks of these structures remain large structure, and exhibit linear polarization.

This paper presents a novel FTRP antenna for misalignment WPT applications. The proposed antenna is constructed based on a  $4 \times 4$  mushroom structure, where  $2 \times 2$  shorting pin is absent to improve the side direction. In order to orient the wave energy equally and achieve uniform power and circular polarization, the antenna combines with a  $4 \times 4$  metasurface. The proposed antenna was computed and verified experimentally. As observed, the structure not only uses the metasurface to achieve the high gain and CP but also obtains uniform power radiation which indicates an advantage over our previous work [17].

## II. ANTENNA DESIGN AND CHARACTERISTICS

### A. RADIATE PRINCIPLE

The scenario and corresponding circuit for creating uniform power are shown in Fig. 1 in order to explain the principle of producing a flat-top radiation antenna. A mushroom structure is used in this work. Due to its ability to function as an electromagnetic band-gap (EBG) structure when combined with a shorting via, the mushroom structure has a number of benefits such as flat-top radiation, side and back-lobe reduction, and ability to suppress the surface wave of both TE and TM polarization [20], [21]. In addition, one of the simplest methods to generate a flat-top beam is to reduce the peak orientation in the 0-degree direction and to increase the radiation intensity in the lateral direction. As illustrated in Fig. 1(a), a metasurface is employed to fulfill this requirement. The metasurface operates as the parasitic element to promote the direct improvement of the wave radiation levels of the mushroom structure.

The total field of the proposed structure can be calculated by two equations following as [17]:

$$\begin{aligned} [E_\phi]_{total} &= [E_\phi]_{Feeding} + (Ae^{j\omega})[E_\phi]_{radiator} + E_\phi\sqrt{\delta D_\phi} \\ [E_\theta]_{total} &= [E_\theta]_{Feeding} + (Ae^{j\omega})[E_\theta]_{radiator} + E_\theta\sqrt{\delta D_\theta}, \end{aligned} \quad (1)$$

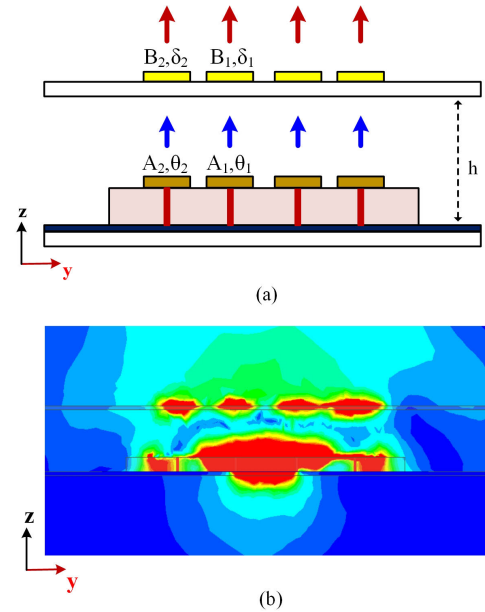


FIGURE 1. (a) Scenario of generating uniform power antenna and (b) The E-field distribution.

where  $E_\phi$  and  $E_\theta$  are two orthogonal components of the electric field, and  $A$  and  $\omega$  are the amplitude and phase, respectively. The additional directivity  $\delta D$  after combining the metasurface was calculated based on the ray-tracking model as [12], [13]

$$\delta D = 10 \log \frac{1 - B^2}{1 + B^2 - 2B \cos(\delta - \pi - h \frac{4\pi}{\lambda} \cos\theta)}, \quad (2)$$

where  $\theta$  is the angle between the unit cell and the vertical, and  $B$  and  $\delta$  are the amplitude and phase of the reflection coefficient, respectively. In order to achieve the maximum power pattern at  $\beta$  direction, the distance  $h$  between the ground plane and metasurface must be satisfied as

$$h = \frac{(2n\pi + \delta - \pi)\lambda}{4\pi \cos\beta}, \quad n = 1, 2, \dots \quad (3)$$

To radiate efficiently and exhibit a low profile, it can be shown that the metasurface should be set up around a quarter wavelength above the ground plane. Furthermore, the figure for electric distribution indicates that the exception is realized based on the principle of generating flat-top radiation, as shown in Fig. 1(b). It can be seen that the proposed antenna is composed of a mushroom structure integrated with a metasurface, which provides a relatively flat amplitude distribution.

The main contribution of this idea is the use of a phase-corrected structure MS, which improves the radiation field uniformity while preserving the radiation characteristics from the mushroom structure. The paper's advantages are a low profile, high gain, uniform power radiation that is superior to most previous designs.

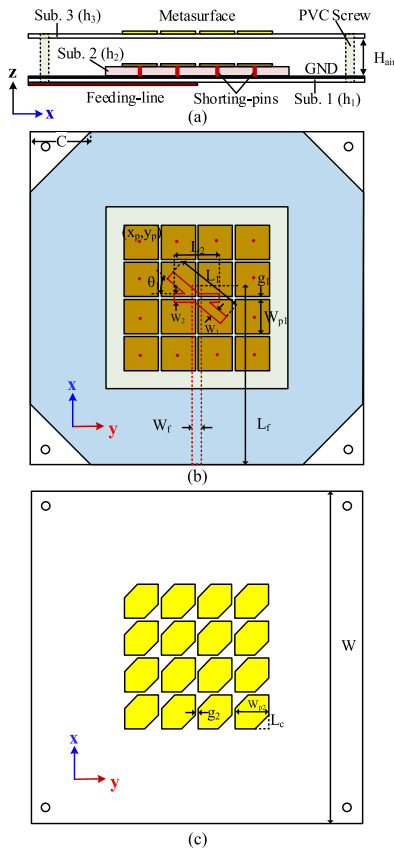


FIGURE 2. Configuration of the proposed FTRP antenna (a) side view, (b) top view of the mushroom structure, and (c) top view of the MS.

B. ANTENNA GEOMETRY

Fig. 2 illustrates the configuration of the proposed FTRP antenna, which comprises an aperture coupled feed, a mushroom structure, a metasurface, and a subminiature version A (SMA) connector. The structure is designed on three substrate layers, which are Taconic TLY-5 sheets (relative dielectric constant of 2.2 and loss tangent of 0.0009). The aperture-coupled feed is printed on both sides of the bottom substrate with thickness of 0.8mm, and the mushroom structure is located directly above the substrate with thickness of 3.2mm. The mushroom structure is composed of 4 × 4 square unit cells with the size  $W_{p1}$  of about a quarter wavelength. Moreover, we can utilize the mushroom structure antenna incorporating with metasurface, where the each unit cell is chosen to be a same size as radiating elements to direct the electric field. Besides, the ground plane size is optimized around  $2\lambda_0$  to obtain flat-top radiation. An air gap with a quarter wavelength is inserted between two layers to obtain the high gain and low profile. Besides, the proposed antenna was computed by using ANSYS Electronics Desktop and the geometry parameter values are listed as follows:  $L_1 = 23$ ,  $L_2 = 15$ ,  $L_c = 4.5$ ,  $L_f = 59$ ,  $W = 110$ ,  $W_1 = 3$ ,  $W_2 = 3$ ,  $C = 20$ ,  $W_{p1} = 11.5$ ,  $W_{p2} = 11.5$ ,  $x_p = 19$ ,  $y_p = 19.3$ ,  $g_1 = 1.1$ ,  $g_2 = 1.1$ ,  $H_{air} = 13$ ,  $h_1 = 0.8$ ,  $h_2 = 3.2$ ,  $h_3 = 0.8$ ,  $\theta_1 = 40^\circ$ . (Unit mm)

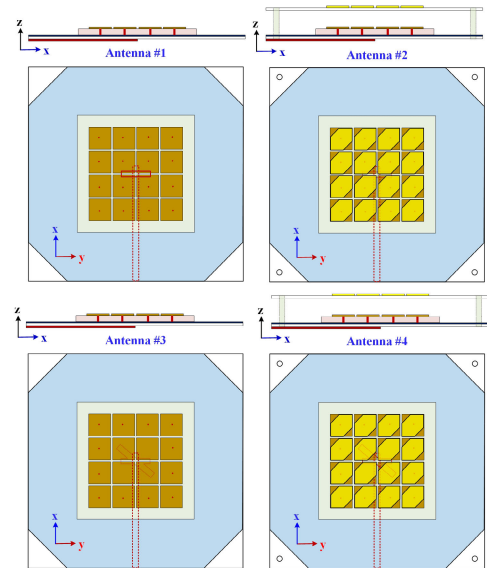


FIGURE 3. Details in design steps of proposed antenna.

C. DESIGN EVOLUTION

The combination of the mushroom antenna and metasurface provides a flat-top radiation enhancement, surpassing previous results found in [15] and [17]. The proposed antenna is obtained by considering the reflection coefficient, and especially the flat-top radiation pattern. Throughout the design process, four distinct antenna configurations are developed in order to achieve the best performance characteristics, as illustrated in Fig. 3.

Antenna #1 is designed with an increased number of mushroom units and using four corner cuts on the ground plane, utilizing the principle established in [17] to create an FTRP and improve gain. In the next stage of development, a metasurface consisting of a 4 × 4 unit cell with two cut corners on an additional substrate is introduced in antenna #2. The purpose of this is to minimize the peak directivity at  $0^\circ$  and to enhance gain in surrounding directions by using the same size of unit cells of the mushroom structure. In antenna #3, the addition of  $\theta_1$ -rotated ground slots produces the CP characteristic, while simultaneously removing the 2 × 2 shorting via in the middle of the radiator to improve the impedance bandwidth. After thorough simulations using ANSYS Electronics Desktop, the final design is realized to be a combination of the antenna #2 and the antenna #3. Each unit cell is used with the same size as the radiator of the mushroom structure. All three configurations are simulated under identical conditions in terms of overall size, height, type of substrate, and parameter values, as listed in Table 1.

The performances of each antenna geometry are shown in Fig. 4. Antenna #1 exhibits poor impedance matching and an approximately 11 dB improvement in gain when the number of mushroom structures is increased, but the flat-top gain is suppressed. Antenna #2 employs a metasurface, which results in a gradually 10 dBi flat-top beamwidth

TABLE 1. Comparison with latest relevant works.

Ref.	Configuration	1-dB beamwidth (E-plane/H-plane)	Polarization	Gain (dBi)	Overall Size ( $\lambda_0^3$ )
[13]	Fabry-Pérot Cavity	58°/58° (2dB)	LP	11	2.37 × 2.37 × 0.67
[14]	Leaky-wave	40°/40°	LP	12.1	13.6 × 13.6 × 1
[15]	Array	24°/*	LP	11.8	7.38 × 1.3 × 0.17
[16]	Dielectric Resonator	54°/58°	CP	8.5	2.7 × 1.5 × 0.8
[17]	Patch	56.4°/58.9°	CP	8.5	1.93 × 1.93 × 0.075
[18]	GIMS Lens	*/34°	LP	13.36	4 × 4 × 0.54
[19]	Lens	80°/80°	LP	10	$\pi \times 3.5 \times 3.5 \times 4$
Prop.	Patch, Meta	35°/38°	CP	10.4	2.13 × 2.13 × 0.288

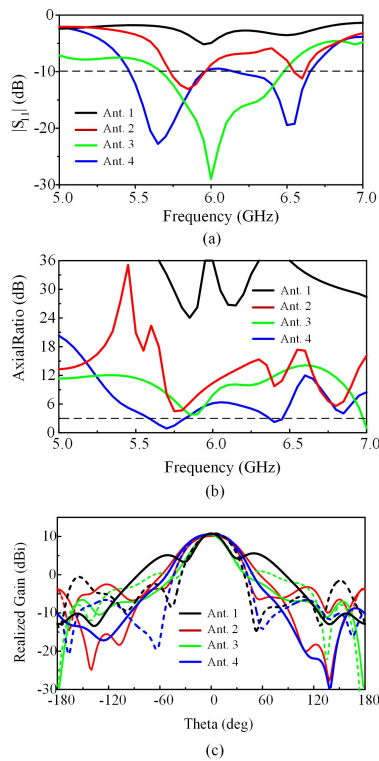


FIGURE 4. (a) Reflection coefficient ( $S_{11}$ ), (b) AR and (c) total gain (“dot-line: E plane, line: H plane”).

in the H-plane and there is an optimal matching impedance at 5.8 GHz. However, the axial ratio (AR) is still higher than 3 dB. Moreover, antenna #3 shows a wide bandwidth from 5.67 GHz to 6.48 GHz, and the axial ratio value is approximately 3 dB at 5.9 GHz. Finally, antenna #4 yields an impedance bandwidth ( $S_{11} < -10$  dB) of 19.67% (5.5-6.7 GHz) with CP characteristic at 5.8GHz. The proposed antenna also achieves a 1-dB beamwidth of larger than 36° in both the E and H planes.

As aforementioned, the additional directivity of the metasurface is directly influenced by the distance  $h$  between the ground and the metasurface. Therefore, the  $S_{11}$ , AR,

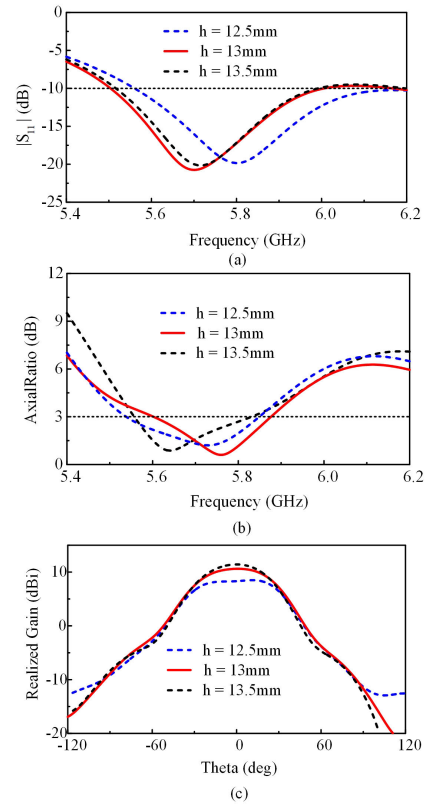


FIGURE 5. Simulated results on  $S_{11}$ , AR, and realized gain values according to air-gap ( $h$ ).

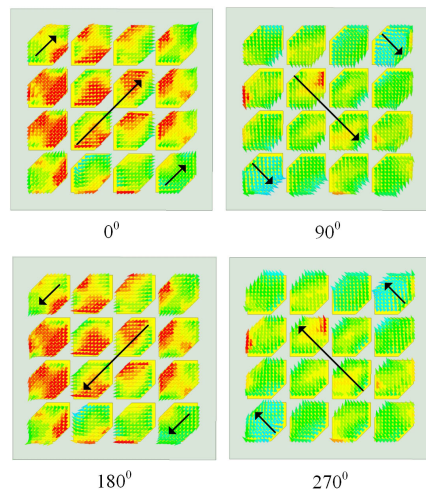


FIGURE 6. Current distributions on the metasurface at 5.8 GHz.

gain radiation subject to the distance  $h$  are evaluated, as depicted in Fig. 5. It can be observed that good impedance matching is obtained for the whole situation. For the case where  $h$  is adjusted to 13 mm (approximately a quarter wavelength), the AR and 3 dB FTRP simultaneously achieve the best state.

Diagrams with current distribution are illustrated to clarify the circular polarization of the proposed antenna, as shown in Fig. 6. The current directions are supported with additional

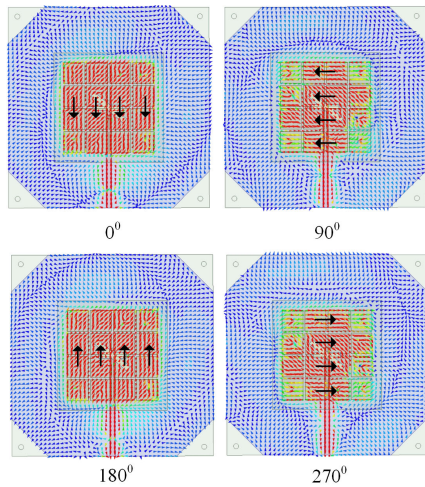


FIGURE 7. Current distributions on the ground plane and radiator at 5.8 GHz.

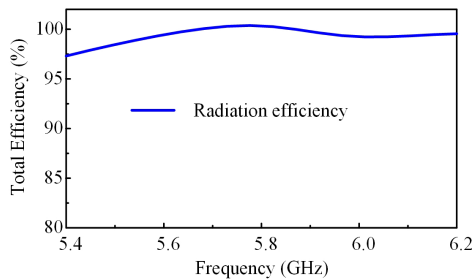


FIGURE 8. Total efficiency of the antenna.

highlighted black arrows. In the initial phase, the current intensity on the metasurface is followed upward  $45^\circ$  direction, whereas the figure for a phase of  $90^\circ$  indicates that current density is observed downward  $45^\circ$  direction. The current distribution on the ground plane and radiator with the phase current directed along the x and y axes, is shown in Fig. 7. Moreover, it can be seen that the current dispersion is most concentrated on the region with a mushroom structure. Finally, the figure for the total efficiency of the proposed structure is illustrated in Fig. 8. It is indicated that the radiation efficiency is higher than 97% at the considered frequency range. Hence, the FTRP antenna can radiate power effectively.

### III. MEASUREMENTS AND EXPERIMENTS

#### A. FABRICATION AND MEASUREMENT RESULTS

For verifying the simulation results, the proposed antenna is fabricated with an overall size of  $2.13\lambda_0 \times 2.13\lambda_0 \times 0.228\lambda_0$ , as depicted in Fig. 9. The antenna is connected to a vector network analyzer (Agilent 8719D) to realize the reflection coefficient results. It is shown in Fig. 10(a) that the measured results obtained the impedance bandwidth ( $< -10$  dB) is 7% from 5.6 to 5.9 GHz, whereas the simulated one is 8.69% (5.5–6GHz). Furthermore, a far-field measurement is set up

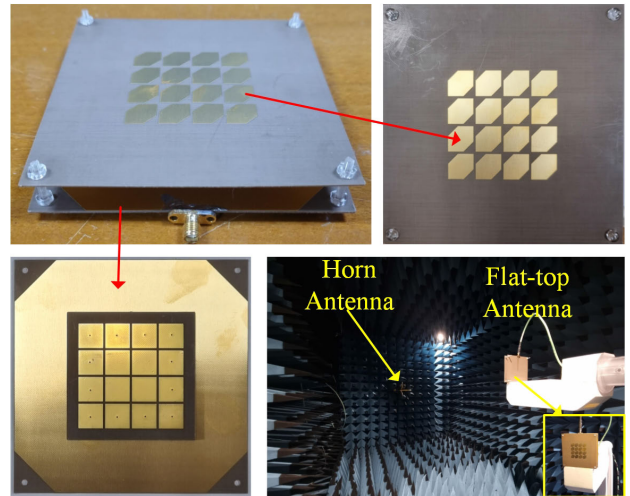


FIGURE 9. Fabricated geometry of the proposed FTRP antenna.

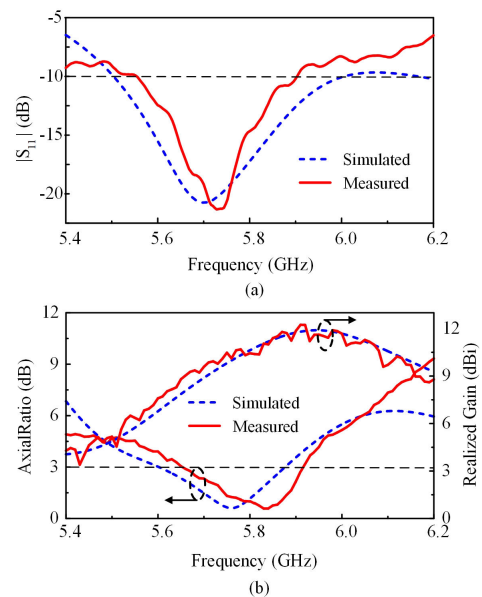


FIGURE 10. Simulated and measured results. (a)  $|S_{11}|$ , and (b) AR and realized gain values.

with an anechoic chamber environment to evaluate the two-dimension (2D) radiation patterns. As indicated in 10(b), the axial-ratio value (AR) has approximately 0 dB for simulated result at 5.8GHz and yields 1.4 dB for measured one. Besides, the realized gain is also measured, obtaining a peak gain of 10.4 dBi, which is 0.5 dBi lower than simulation. The deviation occurs when the substrate layers are stacked, which makes the spacing between them incorrect.

On the other hand, the realized radiation pattern of the proposed structure versus angle is evaluated in Fig. 11. There is a good agreement between measured and simulated results. It is clear that the measured LHCP gain is realized with the maximum directivity of 10.4 dBi in both E and H planes, whereas the simulated one achieves the maximum of

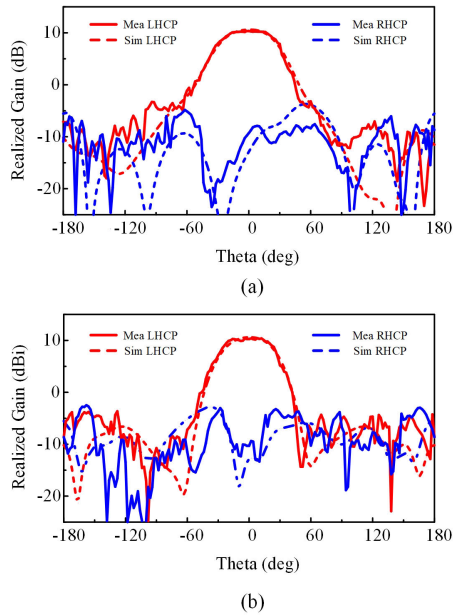


FIGURE 11. Simulated and measured results of the proposed antenna at 5.8 GHz (a) E plane pattern (b) H plane pattern.

10.88 dBi. In addition, the cross left-hand circular polarization is less than -20 dB, and the 1 dB beamwidth in the E and H planes is 36° and 38°, respectively.

**B. COMPARISON AND DISCUSSION**

Table 1 summarizes the advantages of the proposed FTRP antenna compared to the other related state-of-the-art studies. The proposed antenna is highlighted for the easy observation of highly efficient FTRP, CP, and low profile. Specifically, the proposed design obtains a smaller in overall size and a CP characteristic relative to the PFC and LWAs methods in [13] and [14]. In particular, with the support of the metasurface, the proposed design yields an performance improvement as compared to [15], [16], and [17], which are smaller size, and higher gain. The antenna using metasurface in [18] and [19] achieves good results in high gain and wide beamwidth, but the compactless structure size and linear polarization are disadvantageous.

**C. MICROWAVE POWER TRANSMISSION SYSTEM**

For further verification, a MPT system is built to evaluate the flat-top beam antenna, as depicted in Fig. 12. The proposed antenna is designed in the previous sections and acts as a transmitting antenna. The FTRP antenna is linked to an amplifier (SN192902007), RF signal generator (Agilent N5182A), and DC power supply (Aligent E3633A) on the transmitter side, where the radiated power at the transmitting antenna is restricted to 30dBm (1 W) because the system is executed under FCC regulations that are designed to safeguard the human body. At the receiver side, a rectenna is used in [4], which is composed of a receiving antenna and a rectifier for verifying the received power. The receiver is placed

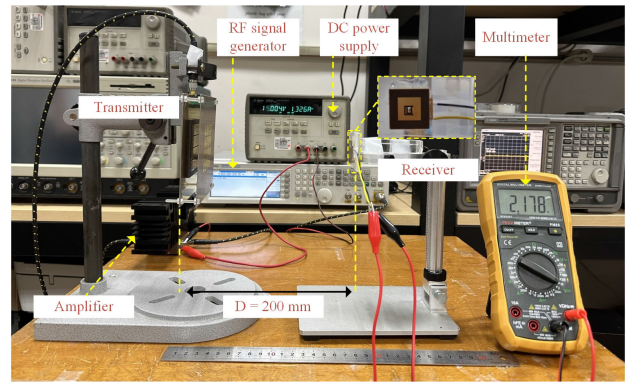


FIGURE 12. Experimental setup of the MPT system.

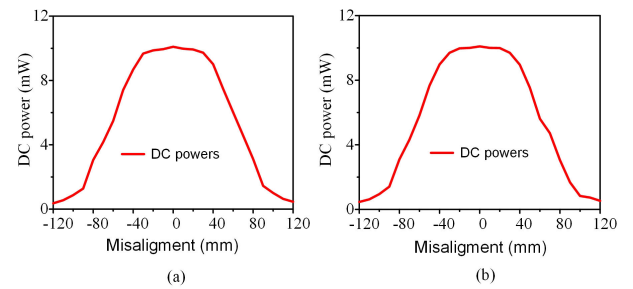


FIGURE 13. Output power at receiver (a) xoz plane (b) yoz plane.

in the light of sight with a transmitter at a distance of 200 mm because it is related to the sensitivity. The distance is fixed so that the energy received at the receiver is within the dynamic range of the rectifier for the highest power conversion efficiency achievement. The output load of the rectifier connects to a Digital Multimeter to observe the output voltage. As can be seen, the measured received power reaches a maximum value of approximately 10mW, which corresponds to the output voltage of 2.178V displayed on the multimeter and is calculated based on a resistive load of 470Ω. To demonstrate the uniform wireless powering capability of the transmitting antenna, the dc output voltage is monitored by varying the lateral misalignment of the rectenna. Fig. 13 provides the output DC power at the receiver for both planes in the case of lateral misalignment within a 120 mm offset. The received output power is confirmed with the radiation pattern of the FTRP antenna. Specifically, the output dc power is almost constant for the lateral movement diameter of 80mm in both the E and H planes. As a result, the metasurface is used to create a direct electromagnetic field direction, which is a way to improve WPT efficiency while maintaining uniform radiation and enabling gain enhancement.

**IV. CONCLUSION**

In this letter, we have presented a high-gain uniform power antenna with metasurface for MPT applications. It comprises a 4 × 4 mushrooms structure-based aperture coupled feeding and a metasurface to obtain uniform power radiation. The final design with the overall size of 2.13λ<sub>0</sub> × 2.13λ<sub>0</sub> × 0.228λ<sub>0</sub> achieves a measured bandwidth of 8.69 %

(5.5–6 GHz), a high gain of 10.4 dBi with flat-top radiation pattern wider than  $36^\circ$  in both E and H planes. The proposed FTRP antenna is also achieved several advantages with features such as high gain, uniform power radiation, and CP. In the MPT experiment, the system shows that the rectenna can receive 10mW uniform power at a distance of 200 mm with a lateral misalignment diameter of 80 mm. With the above advantage, the proposed antenna can be a good candidate for the MPT applications for charging multiple devices or moving devices.

## REFERENCES

- [1] Z. Zhang, H. Pang, A. Georgiadis, and C. Cecati, "Wireless power transfer—An overview," *IEEE Trans. Ind. Electron.*, vol. 66, no. 2, pp. 1044–1058, Feb. 2019.
- [2] Z.-X. Du, S. F. Bo, Y. F. Cao, J.-H. Ou, and X. Y. Zhang, "Broadband circularly polarized rectenna with wide dynamic-power-range for efficient wireless power transfer," *IEEE Access*, vol. 8, pp. 80561–80571, 2020.
- [3] T. D. P. Perera, D. N. K. Jayakody, S. K. Sharma, S. Chatzinotas, and J. Li, "Simultaneous wireless information and power transfer (SWIPT): Recent advances and future challenges," *IEEE Commun. Surveys Tuts.*, vol. 20, no. 1, pp. 264–302, 1st Quart., 2018.
- [4] D. M. Nguyen, N. D. Au, and C. Seo, "A microwave power transmission system using sequential phase ring antenna and inverted class F rectenna," *IEEE Access*, vol. 9, pp. 134163–134173, 2021.
- [5] Z.-C. Hao, M. He, and W. Hong, "Design of a millimeter-wave high angle selectivity shaped-beam conformal array antenna using hybrid genetic/space mapping method," *IEEE Antennas Wireless Propag. Lett.*, vol. 15, pp. 1208–1212, 2016.
- [6] F. M. Monavar, S. Shamsinejad, R. Mirzavand, J. Melzer, and P. Mousavi, "Beam-steering SIW leaky-wave subarray with flat-topped footprint for 5G applications," *IEEE Trans. Antennas Propag.*, vol. 65, no. 3, pp. 1108–1120, Mar. 2017.
- [7] N. Takabayashi, K. Kawai, M. Mase, N. Shinohara, and T. Mitani, "Large-scale sequentially-fed array antenna radiating flat-top beam for microwave power transmission to drones," *IEEE J. Microw.*, vol. 2, no. 2, pp. 297–306, Apr. 2022.
- [8] Y. Xu, X. Shi, W. Li, and J. Xu, "Flat-top beampattern synthesis in range and angle domains for frequency diverse array via second-order cone programming," *IEEE Antennas Wireless Propag. Lett.*, vol. 15, pp. 1479–1482, 2016.
- [9] L. Sun, S.-G. Zhou, and G.-X. Zhang, "Synthesis method of an orthogonal beamforming network with arbitrary ports for shaped beams," *IEEE Trans. Antennas Propag.*, vol. 70, no. 6, pp. 4794–4802, Jun. 2022.
- [10] S. Dai, M. Li, Q. H. Abbasi, and M. A. Imran, "A zero placement algorithm for synthesis of flat top beam pattern with low sidelobe level," *IEEE Access*, vol. 8, pp. 225935–225944, 2020.
- [11] J. Lipor, S. Ahmed, and M.-S. Alouini, "Fourier-based transmit beam-pattern design using MIMO radar," *IEEE Trans. Signal Process.*, vol. 62, no. 9, pp. 2226–2235, May 2014.
- [12] G. V. Trentini, "Partially reflecting sheet arrays," *IRE Trans. Antennas Propag.*, vol. AP-4, no. 4, pp. 666–671, Oct. 1956.
- [13] X. Ran, X.-H. Wang, Y.-D. Hu, S.-W. Qu, and B.-Z. Wang, "Dual-polarized nonuniform Fabry–Pérot cavity antenna with flat-topped radiation pattern," *IEEE Antennas Wireless Propag. Lett.*, vol. 21, no. 5, pp. 1060–1064, May 2022.
- [14] F. Scattone, M. Ettore, R. Sauleau, N. T. Nguyen, and N. J. G. Fonseca, "Optimization procedure for planar leaky-wave antennas with flat-topped radiation patterns," *IEEE Trans. Antennas Propag.*, vol. 63, no. 12, pp. 5854–5859, Dec. 2015.
- [15] Z. Zhang, N. Liu, S. Zuo, Y. Li, and G. Fu, "Wideband circularly polarised array antenna with flat-top beam pattern," *IET Microw., Antennas Propag.*, vol. 9, no. 8, pp. 755–761, Jun. 2015.
- [16] C. K. Wang, B. J. Xiang, S. Y. Zheng, K. W. Leung, W. S. Chan, and Y. A. Liu, "A wireless power transmitter with uniform power transfer coverage," *IEEE Trans. Ind. Electron.*, vol. 68, no. 11, pp. 10709–10717, Nov. 2021.
- [17] D. M. Nguyen, N. D. Au, and C. Seo, "Aperture-coupled patch antenna with flat-top beam for microwave power transmission," *IEEE Antennas Wireless Propag. Lett.*, vol. 21, no. 10, pp. 2130–2134, Oct. 2022.
- [18] A. K. Singh, M. P. Abegaonkar, and S. K. Koul, "Wide angle beam steerable high gain flat top beam antenna using graded index metasurface lens," *IEEE Trans. Antennas Propag.*, vol. 67, no. 10, pp. 6334–6343, Oct. 2019.
- [19] N. T. Nguyen, R. Sauleau, and L. L. Coq, "Reduced-size double-shell lens antenna with flat-top radiation pattern for indoor communications at millimeter waves," *IEEE Trans. Antennas Propag.*, vol. 59, no. 6, pp. 2424–2429, Jun. 2011.
- [20] M. J. Al-Hasan, T. A. Denidni, and A. R. Sebak, "Millimeter-wave EBG-based aperture-coupled dielectric resonator antenna," *IEEE Trans. Antennas Propag.*, vol. 61, no. 8, pp. 4354–4357, Aug. 2013.
- [21] T. A. Denidni, Y. Coulibaly, and H. Boutayeb, "Hybrid dielectric resonator antenna with circular mushroom-like structure for gain improvement," *IEEE Trans. Antennas Propag.*, vol. 57, no. 4, pp. 1043–1049, Apr. 2009.



**DANH MANH NGUYEN** received the B.Sc. (Eng.) degree in electronics and telecommunication from the School of Electronics and Telecommunication (SET), Hanoi University of Science and Technology, Hanoi, Vietnam, in 2020, and the M.S. degree from Soongsil University, Seoul, South Korea, in 2022, where he is currently pursuing the Ph.D. degree with the Department of Information Communication, Materials, and Chemistry Convergence Technology. His research interests include high gain antenna, wideband antennas, multiple-polarized antennas, wireless power transfer, and metamaterials.



**DUCDUNG NGUYEN** (Graduate Student Member, IEEE) received the B.S. degree from the School of Electronics and Telecommunications, Vinh University, Nghe An, in 2018. He is currently pursuing the integrated M.S. and Ph.D. degrees with the Department of Information Communication, Materials, and Chemistry Convergence Technology, Soongsil University, Seoul, South Korea. His current research interests include high-gain antenna, power amplifiers, metamaterials, wireless power transfer, and biomedical implantable antenna.



**CHULHUN SEO** (Senior Member, IEEE) received the B.S., M.S., and Ph.D. degrees from Seoul National University, Seoul, South Korea, in 1983, 1985, and 1993, respectively. From 1993 to 1995, he was with the Massachusetts Institute of Technology (MIT), Cambridge, MA, USA, as a Technical Staff Member. From 1993 to 1997, he was an Assistant Professor with Soongsil University, Seoul. From 1999 to 2001, he was a Visiting Professor with MIT. From 1997 to 2004, he was an Assistant Professor with Soongsil University, where he has been a Professor in electronic engineering, since 2004. He is currently the Director of the Wireless Power Transfer Research Center supported by the Korean Ministry of Trade, Industry, and Energy, and the Director of the Metamaterials Research Center, which is supported by the Basic Research Laboratories through NRF grant funded by MSIP. His research interests include wireless communication technologies, RF power amplifiers, and wireless power transfer using meta-materials. He served as the IEEE MTT Korea Chapter Chairperson, from 2011 to 2014.